FLOW FIELD STUDIES USING HOLOGRAPHIC
INTERFEROMETRY AT LANGLEY

A. W. Burner, W. L. Snow, W. K. Goad,
V. T. Helms, and P. B. Gooderum

NASA Langley Research Center
Hampton, Virginia

INTRODUCTION

During the past decade holographic interferometry has largely superseded the classical Mach-Zender interferometer as the interferometric technique with the best potential for measuring density in aerodynamic research facilities. Holographic interferometry is a nonintrusive optical technique which offers the additional capability over conventional interferometry of recording for later reconstruction the flow and no-flow optical fields. It is the interference between these two optical fields which yields fringe shift data necessary for density calculations. This paper traces some of the uses of holographic interferometry at Langley Research Center both for flow visualization and for density field determinations and concludes with the description of recent tests in cryogenic flows at the Langley 0.3-Meter Transonic Cryogenic Tunnel.

HOLOGRAPHIC FLOW VISUALIZATION FROM THE LANGLEY CF_4 TUNNEL

The main use of holography in wind tunnels at Langley has been for flow visualization. Figure 1 is an interferogram made at the Langley Hypersonic CF_4 tunnel of the Shuttle Orbiter nose in Mach 6 flow. The field of view is 40 cm^4 with flow from left to right. Note that the maximum fringe shift is less than 4. Smaller models run at the facility at low freestream density have fringe shifts less than 1.0.
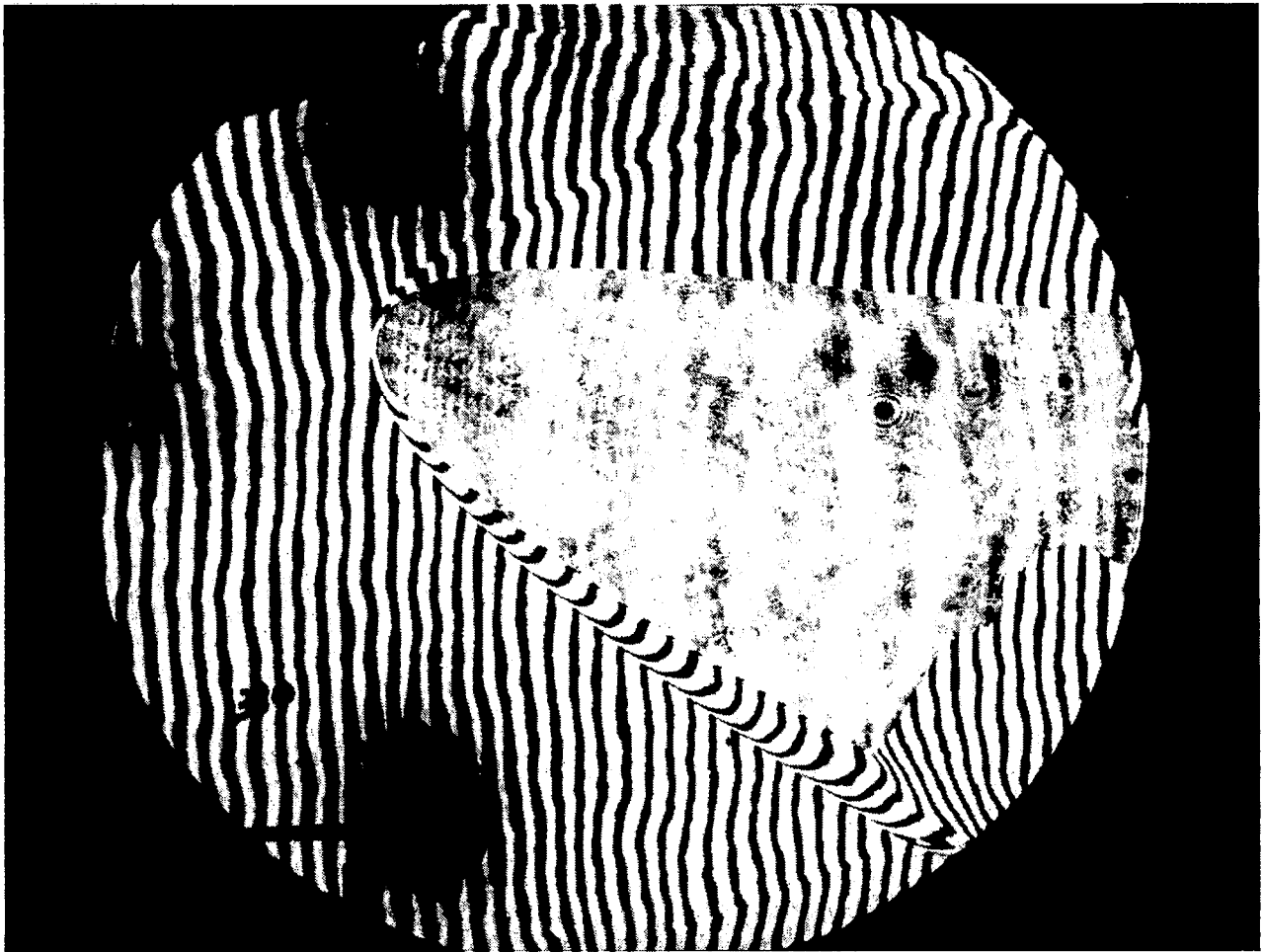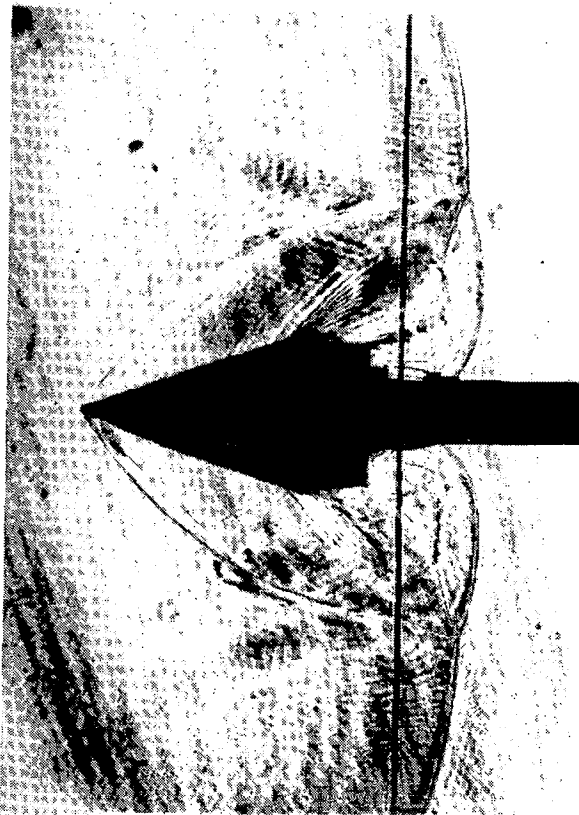

Figure 1

HOLOGRAPHIC FLOW VISUALIZATION FROM THE LANGLEY EXPANSION TUBE

Figure 2 shows a shadowgraph and interferogram of a 20° half-angle wedge from the Langley Expansion Tube. Flow is from left to right. In the expansion tube mode of operation maximum fringe shifts vary from about 0.1 to 2.0. For the hologram of figure 2 the facility was operated as a shock tube which resulted in much higher densities and hence larger fringe shifts than when operated as an expansion tube. The incident shock was recorded before leaving the field of view. Note the formation of a bow shock about the wedge.

(a) Shadowgraph.

(b) Interferogram.

Figure 2

INTERFEROGRAM OF CONE FROM LANGLEY CF_4 TUNNEL

To gain some experience with interferometry, fringe shift measurements have been made on several spheres and sphere-cones run at 0°A-0-A at the CF_4 tunnel. An interferogram of a 7.6 cm base 45° half-angle cone is shown in figure 3. Note that the maximum fringe shift is less than 1.0. In order to obtain more fringe crossings and also to determine the repeatability of a number of fringe shift measurements, the same flow and no-flow holograms were used to generate seven interferograms of slightly different fringe spacing. Fringe shift measurements were then made on each interferogram at 9 x-stations, where x is the distance in the direction of flow from the nose of the model.
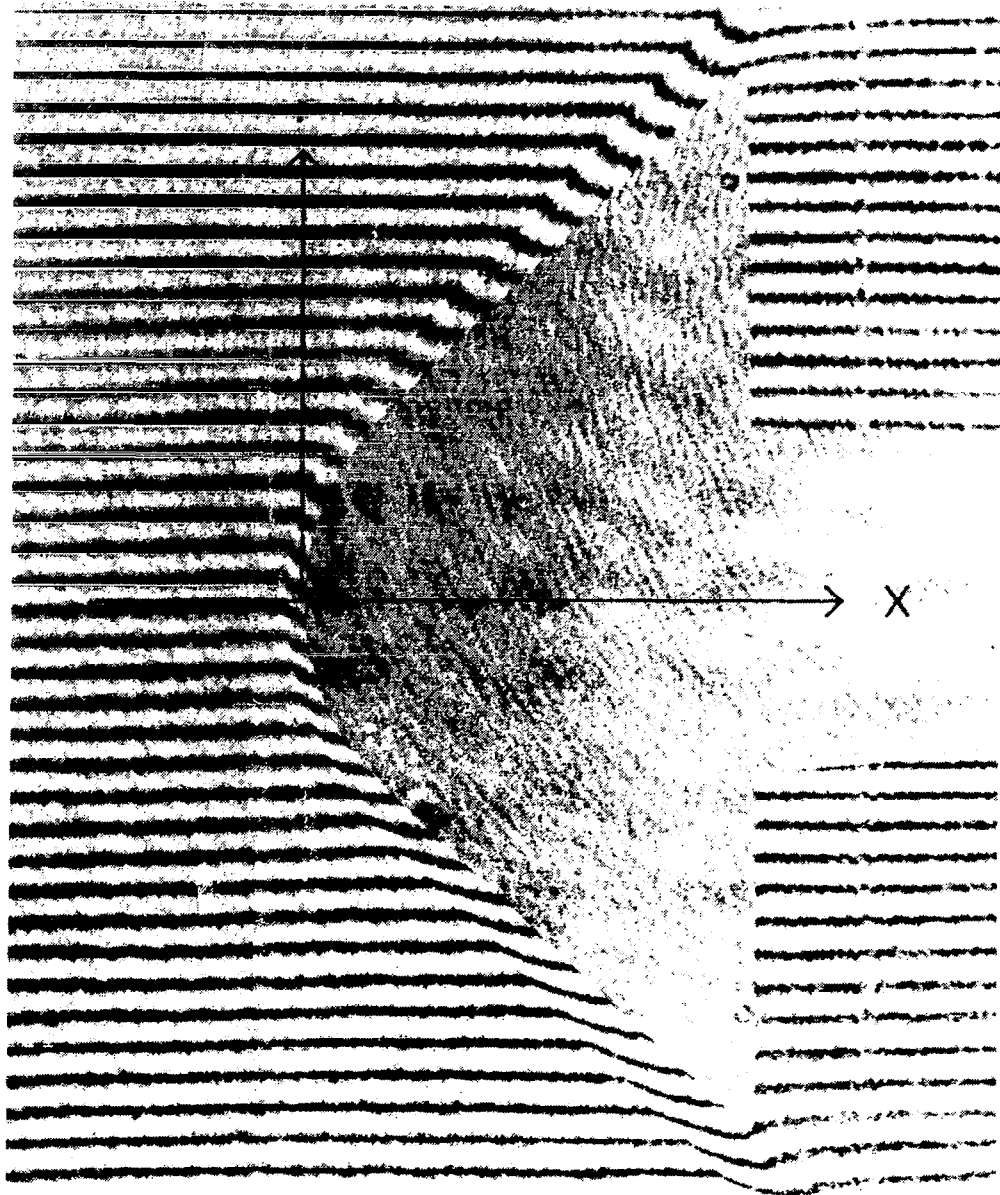

Figure 3

FRINGE SHIFT DATA

In figure 4 fringe shift S is plotted against r, the distance perpendicular
to the flow from the model centerline. The plots are for x-stations slightly
in front of the nose, 60% of the nose-to-base distance, and 95% of the nose-to-base
distance. The solid line on the plots is the theoretical fringe shift curve
calculated from the predicted density field. Note that a comparison of experimental
and theoretical fringe shift curves is an effective way to verify computer codes
which are used to predict density flow fields. This kind of comparison can be made
for asymmetrical flows as well. When comparing experimental and theoretical
fringe shift data it should be remembered that the fringe shift data is
sensitive to interferogram alignment on the digitizing surface, especially so in
front of the nose of the model where the slope of the shock can be very large.
Also uncertainty in the freestream density will lead to uncertainty in the
theoretical fringe shift calculations from the predicted density field. Another
consideration in such comparisons is that the tunnel may be operating in a regime
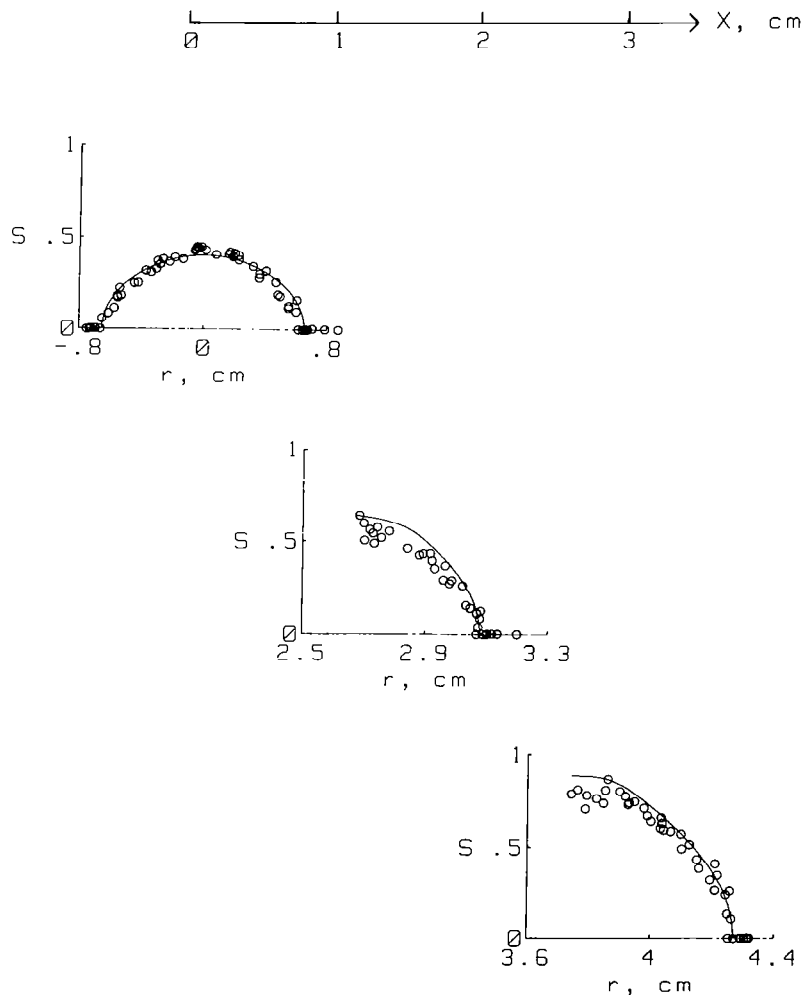where the density predictions are not entirely valid.

Figure 4

DEPENDENCE OF FRINGE SHIFT SHAPE ON DENSITY FUNCTION

Two density functions and their corresponding fringe shifts are presented in figure 5. The density and fringe shift functions are normalized by their on-axis values for comparison. The relatively large scatter of the data in figure 4 makes it difficult to match experimental fringe shift to a particular shape factor. The same problem occurs when attempting to invert the fringe shift data to obtain density since it is necessary to select a "best fit" curve to the experimental data before inversion. In order to use interferograms in which the maximum fringe shift is only 1 or 2 for determining density functions it is necessary that the interferogram be of much higher quality than required for visualization only.
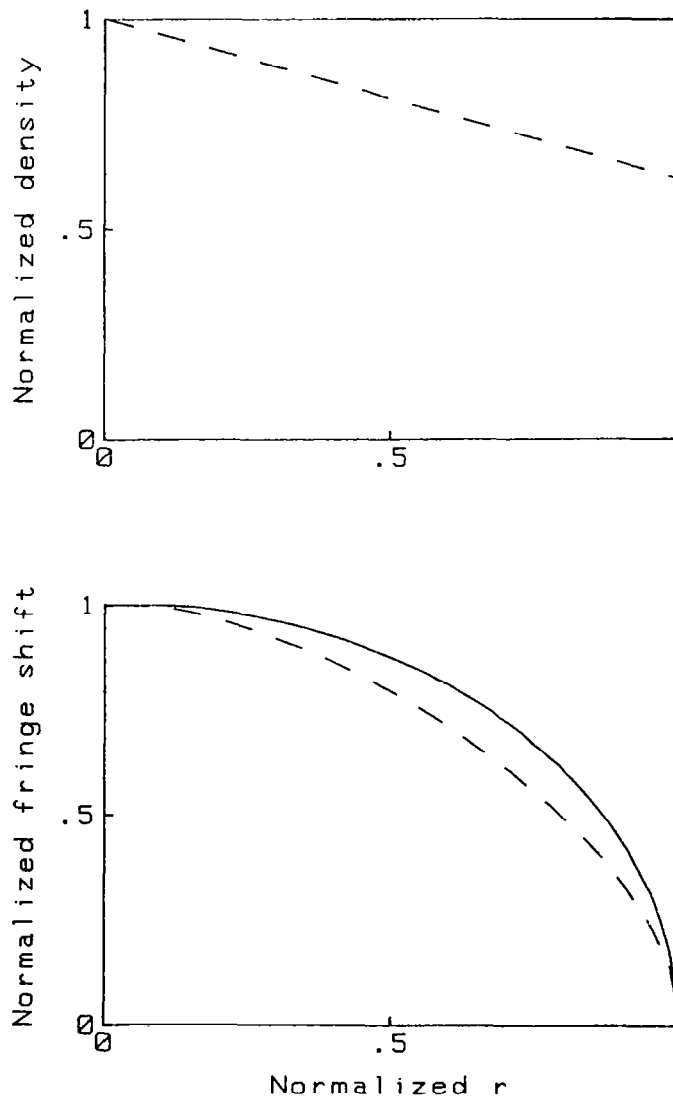

Figure 5

INTERFEROGRAM OF CONE WITH LARGER FRINGE SHIFT

If the fringe shift is larger then requirements on interferogram quality are lessened. Figure 6 is an interferogram of a 13 cm base, 60° half-angle cone for which the maximum fringe shift is about 5 at regions toward the base of the model. The combination of larger base, half-angle, and freestream density resulted in the increased fringe shift for this model.
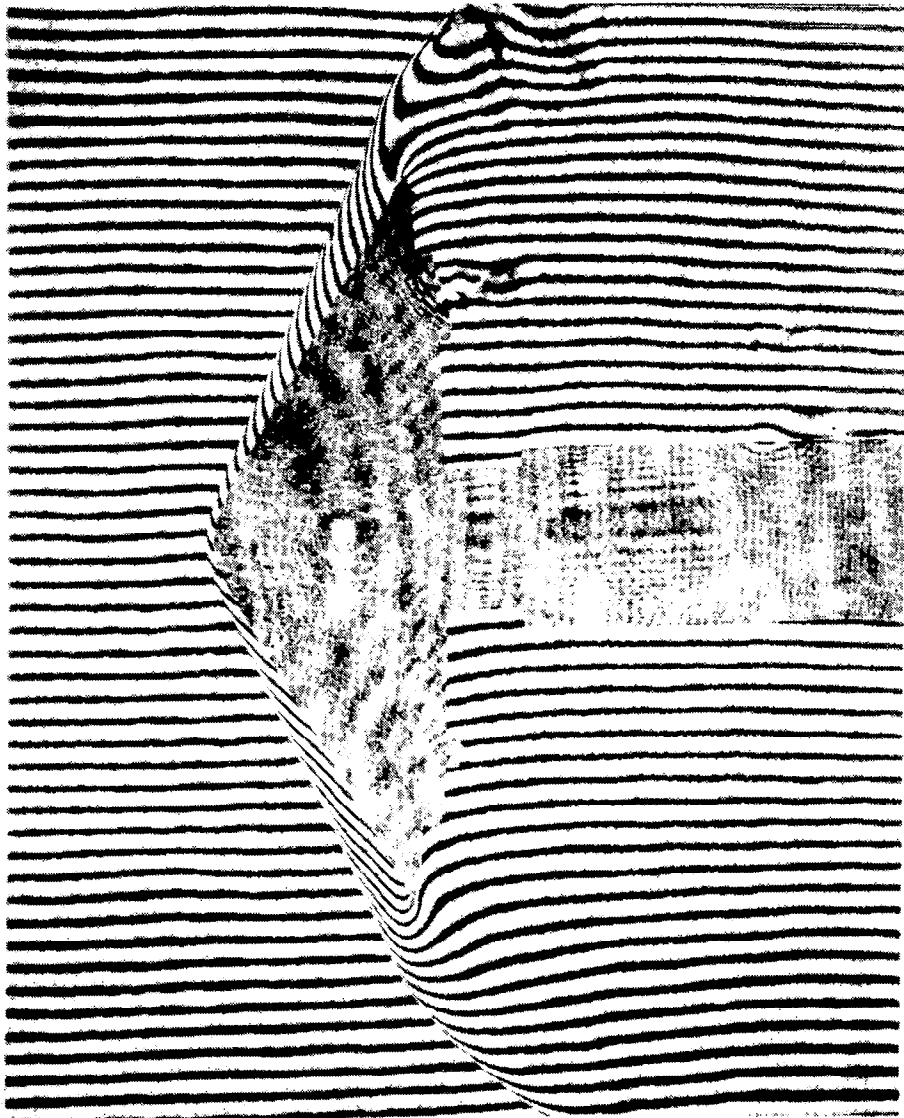

Figure 6

MATCHING OF EXPERIMENTAL FRINGE SHIFT DATA TO SHAPE FACTOR

In figure 7 the experimental fringe shift data taken near the base of the cone of figure 6 is normalized and matched for "best fit" to a theoretical fringe shift shape corresponding to a linear density increase from the shock (located at 7.2 cm from the model centerline) to the model (5.5 cm from model centerline). The density function corresponding to this shape factor is plotted above the fringe shift curve. This density function compared very well with the density function obtained by inverting the fringe shift data. For more complicated density functions a piecewise linear match of fringe shift shape can be made.
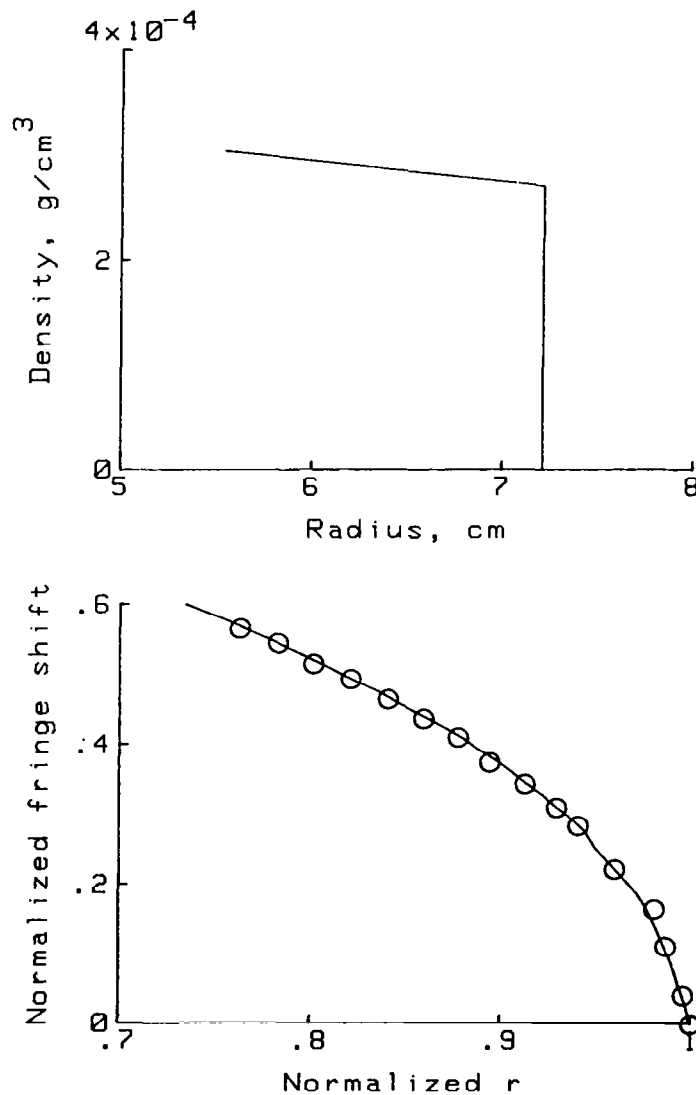

Figure 7

GEOMETRY OF TEST SECTION WINDOWS AND AIRFOIL AT 0.3 METER TCT

The flow field is viewed at the 0.3 meter TCT through "D-Shaped" fused silica test section windows as in figure 8. The lower window edge is 1.9 cm above the centerline of the airfoil so that the airfoil is not visible for flow visualization. For the flow visualization examples in the next two figures, a copper tube purge ring limited the field of view at the top of the photographs. This purge ring vented dry room-temperature N_2 onto the outer plenum windows to prevent condensation on the outer surfaces of the windows as the tunnel temperature was lowered.
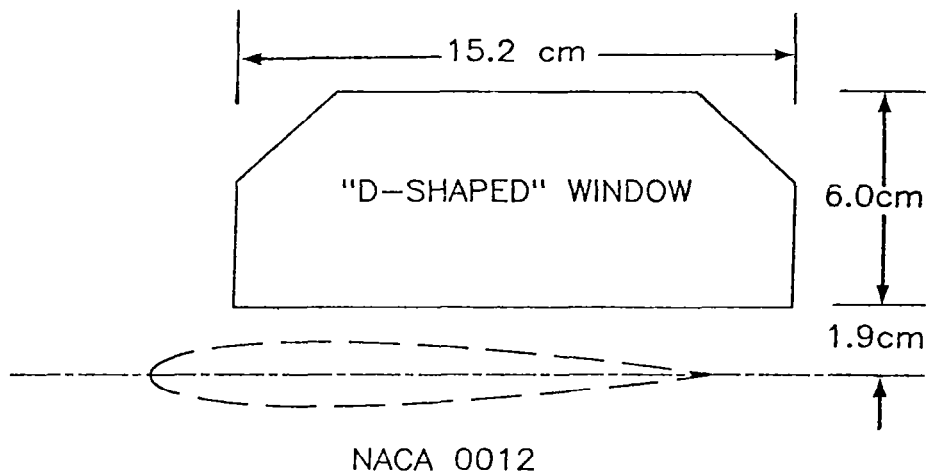

NACA 0012

Figure 8

HOLOGRAPHIC FLOW VISUALIZATION FROM THE 0.3 METER TCT

Figure 9 shows a vertical knife-edge schlieren and interferogram from the same flow hologram recorded at the 0.3 meter TCT. The NACA 0012 airfoil was at 0°A-O-A. The Mach number was 0.77, stagnation temperature was 212 K and stagnation pressure was 2 atm. Flow is from left to right. For these relatively mild conditions the holograms are of excellent quality.
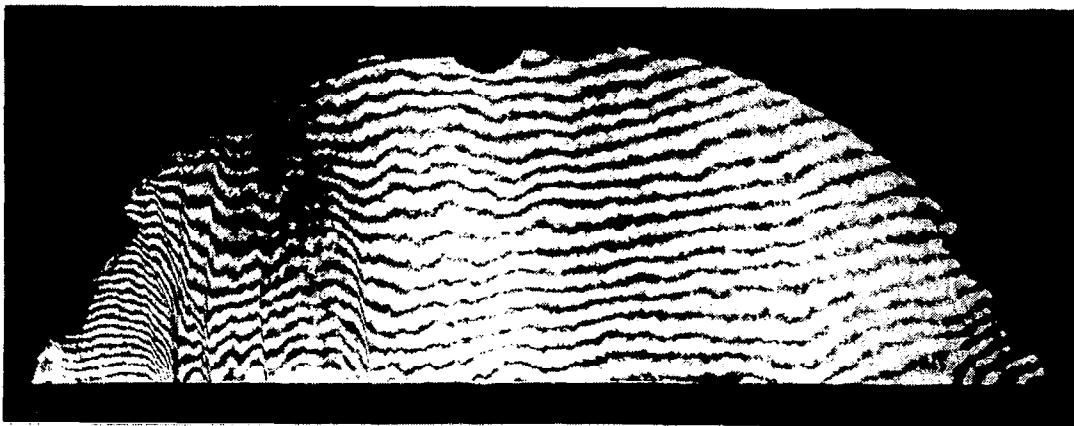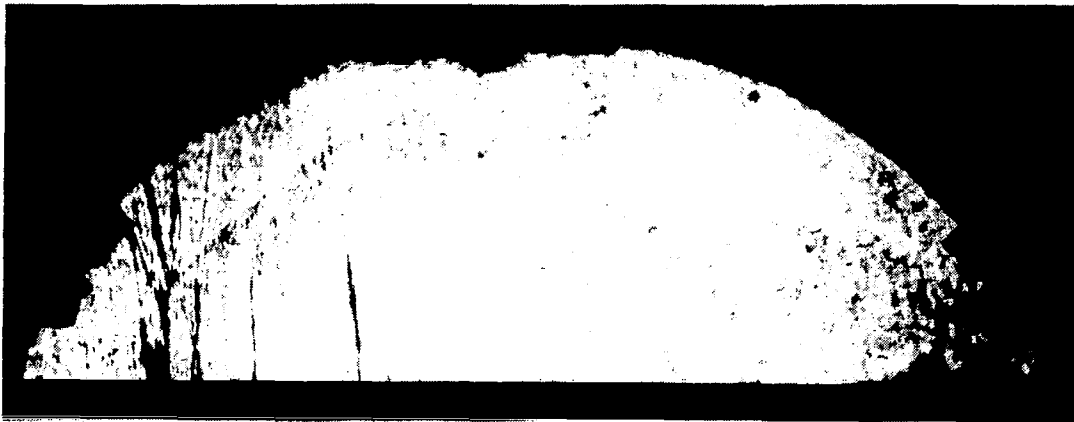
212 K   2 ATM   M = 0.77

Figure 9

HOLOGRAPHIC FLOW VISUALIZATION AT 100 K

Figure 10 is a focused shadowgraph reconstructed from a hologram made at the 0.3 meter TCT. The NACA 0012 airfoil was at 0°A-0-A. The Mach number was 0.77, stagnation temperature was 100 K, and stagnation pressure was 4 atm. Flow is from left to right. Note the grainy appearance of the reconstruction and the very strong (optically) shock. At this condition it has not been possible to produce interferograms. The lowest temperature at which interferograms have been produced is 125 K at 2 atm pressure. At those conditions where interferograms were not possible the spot size at the schlieren focus was noted to be much larger than for those conditions where interferometry was possible. More work is in progress to determine if the degradation noted for these more severe conditions is due to experimental artifact (e.g., condensation on a window) or if it is a fundamental limitation imposed by the low temperature and high pressure.
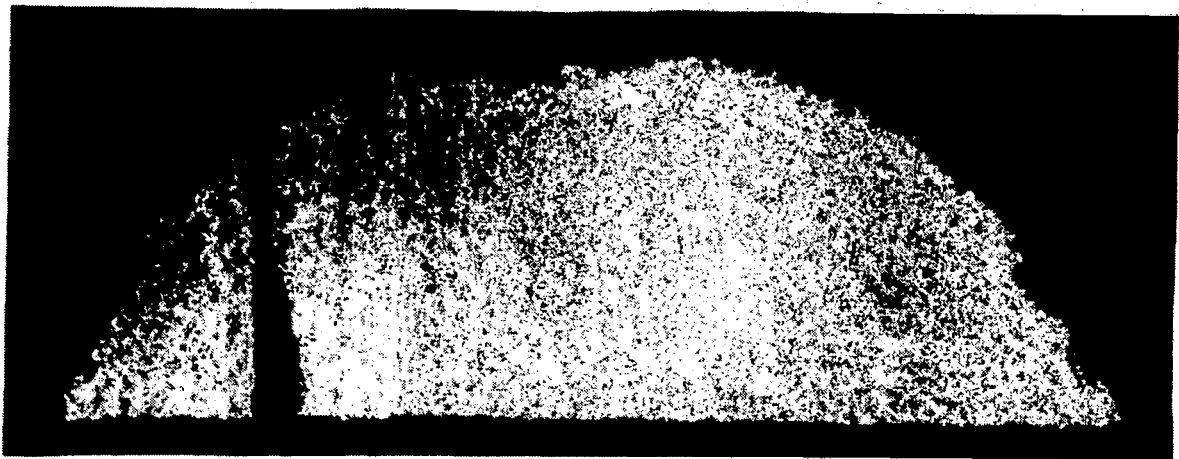
100 K   4 ATM   M = 0.77

Figure 10